Current Biology 22, 1296–1301, July 24, 2012 ©2012 Elsevier Ltd All rights reserved DOI 10.1016/j.cub.2012.04.066

Report

Establishment of Global Patterns of Planar Polarity during Growth of the *Drosophila* Wing Epithelium

Andreas Sagner,[1] Matthias Merkel,[2] Benoit Aigouy,[1,3] Julia Gaebel,[1] Marko Brankatschk,[1] Frank Jülicher,[2,*] and Suzanne Eaton[1,*]

[1]Max Planck Institute of Molecular Cell Biology and Genetics, Pfotenhauerstr. 108, 01307 Dresden, Germany

[2]Max Planck Institute for the Physics of Complex Systems, Nöthnitzer Str. 38, 01187 Dresden, Germany

[3]Génétique Reproduction et Développement, UMR/CNRS 6293, Clermont Université, INSERM U.1103, 28 Place Henri Dunant, 63001 Clermont-Ferrand, France

Summary

Epithelial tissues develop planar polarity that is reflected in the global alignment of hairs and cilia with respect to the tissue axes. The planar cell polarity (PCP) proteins form asymmetric and polarized domains across epithelial junctions that are aligned locally between cells and orient these external structures [1–3]. Although feedback mechanisms can polarize PCP proteins intracellularly and locally align polarity between cells, how global PCP patterns are specified is not understood. It has been proposed that the graded distribution of a biasing factor could guide long-range PCP [4, 5]. However, we recently identified epithelial morphogenesis as a mechanism that can reorganize global PCP patterns; in the *Drosophila* pupal wing, oriented cell divisions and rearrangements reorient PCP from a margin-oriented pattern to one that points distally [6]. Here, we use quantitative image analysis to study how PCP patterns first emerge in the wing. PCP appears during larval growth and is spatially oriented through the activities of three organizer regions that control disc growth and patterning. Flattening morphogen gradients emanating from these regions does not reduce intracellular polarity but distorts growth and alters specific features of the PCP pattern. Thus, PCP may be guided by morphogenesis rather than morphogen gradients.

Results and Discussion

Global PCP Emerges during Growth and Aligns with Organizer Regions

To study the emergence of polarity in the wing disc, we quantified the subcellular distribution of the PCP proteins Flamingo (Fmi) and Prickle (Pk). We calculated planar cell polarity (PCP) nematics based on Fmi staining [6] and PCP vectors based on the perimeter intensity of EGFP::Pk clones (Figures 1A–1C′; see also Figures S1A and S1B available online). At 72 hr after egg laying (hAEL), the wing pouch has just been specified and is small [7]. EGFP::Pk localizes to punctate structures at the cell cortex that are asymmetrically distributed in some cells, but PCP vectors exhibit no long-range alignment (Figures S1D–S1G). By 96 hAEL, PCP vector magnitude increases (Figure S1C) and a global pattern emerges (Figures S1H–S1K). Later, PCP vector magnitude increases further (Figure S1C) and the same global polarity pattern is clearly apparent (Figures 1D–1F). It is oriented with respect to three signaling centers: the dorsal-ventral (DV) boundary (where Wingless [Wg] and Notch signaling occur), the anterior-posterior (AP) compartment boundary (where Hedgehog [Hh] and Decapentaplegic [Dpp] signaling occur), and with respect to the hinge fold (where levels of the atypical Cadherin Dachsous [Ds] change sharply).

PCP vectors in the wing pouch near the hinge fold point away from it toward the center of the pouch. Within the Wg expression domain at the DV boundary, PCP vectors parallel the DV boundary and point toward the AP boundary (Figures 1D–1F, red arrows, lines). Just outside this domain, PCP nematics and vectors turn sharply to point toward the DV boundary in central regions of the wing pouch. However, where the DV boundary intersects the hinge-pouch interface, they remain parallel to the DV boundary over larger distances such that PCP vectors orient away from the hinge around the entire perimeter of the wing pouch (Figures 1D–1F).

The AP boundary is associated with sharp reorientations of PCP. First, PCP vectors that parallel the DV boundary point toward the AP boundary in both anterior and posterior compartments (Figure 1E). Second, although PCP vectors in the central wing pouch are generally orthogonal to the DV boundary, they deflect toward the AP boundary where Hh signaling is most active (as defined by upregulation of the Hh receptor Patched [Ptc]) (Figures 1D–1F, blue lines, arrows, and Figure S1I). On either side of this region, PCP vectors turn sharply to realign parallel to the AP boundary. Third, PCP vectors in the hinge point away from the AP boundary and align parallel to the hinge fold (Figures 1D–1F, orange lines, arrows).

Fat and Dachsous Orient PCP near the Hinge

The atypical Cadherins Fat (Ft) and Ds limit disc growth and orient growth perpendicular to the hinge [8, 9]. Their loss perturbs the PCP pattern in pupal wings and alters hair polarity [10]. To investigate whether they influence the larval pattern, we quantified PCP in *ft* and *ds* mutant discs (Figures 2B–2D). The PCP pattern is similar to wild-type (WT) in the central wing pouch but altered in proximal regions close to the hinge fold (Figure 2). Polarity vectors deviate from their normal orientation (away from the hinge fold) in many regions of the proximal wing pouch. This is especially clear near the intersection of the DV boundary with the hinge—here, PCP vectors orient toward the DV boundary rather than away from the hinge (Figure 2; Figures S2A–SA″). Furthermore, near the AP boundary, vectors form a reproducible point defect, with vectors pointing away from the defect center (Figure 2, red arrows in Figures S2B–S2C′).

After pupariation, morphogenesis reshapes the wing disc, apposing its dorsal and ventral surfaces such that the DV boundary defines the margin of the wing blade (Figure S2F). During reshaping the PCP pattern evolves, but specific local features are retained through pupal development (Figures S2F–S2M′). Consistent with this, hair polarity in *ds* adult wings reflects the perturbed larval pattern (Figure S2E); hairs in the

*Correspondence: julicher@pks.mpg.de (F.J.), eaton@mpi-cbg.de (S.E.)

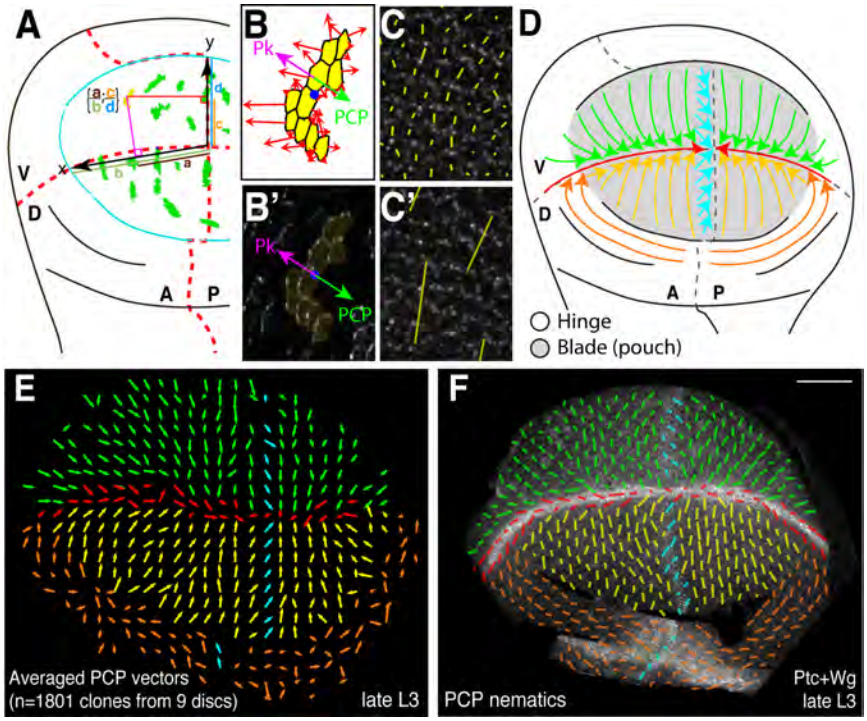

Figure 1. Development of the PCP Pattern

(A) Cartoon of a wing disc with EGFP::Pk clones (green). AP and DV boundaries (red dashed lines) and the hinge/pouch interface (blue line) define a coordinate system. The intersection of AP and DV boundaries defines the origin. Lines running between the origin and the intersection of AP and DV boundaries with the hinge define x and y axes and define lengths b and d. Clone coordinates are determined by calculating normal vectors to the x and y axes that intersect the clone's center of mass. Intersections of normal vectors with the x and y axes define the lengths a and c. Normalized clone coordinates are calculated as (a/b; c/d). This allows averaging of many clones on an average disc coordinate system.

(B and B′) Quantifying and averaging polarity vectors in the wing disc. To calculate clone polarity, we scaled a normal vector defined for each cell boundary along the clone interface by the sum intensity of EGFP::Pk along the cell boundary (red). Vectors are summed and normalized to total EGFP::Pk intensity along the clone interface defining a vector that represents the magnitude and orientation of EGFP::Pk polarity (magenta). We define the PCP vector (green) as the vector with opposite direction but same length as the EGFP::Pk polarity vector.

(C and C′) Single cell nematics (C) or locally averaged nematics (C′) overlaid on Fmi staining of a late third-instar wing disc. Nematics are tensorial objects defined based on the perimeter intensity of PCP protein staining. They are used to characterize strength and orientation of the polarity axis in a single cell without specifying its vector direction. Nematics are visualized by lines. Line length represents the magnitude and line orientation represents the axis of polarity. They can be locally averaged to quantify polarity in groups of cells (see Supplemental Information).

(D) Cartoon illustrating the PCP pattern in a late third-instar wing disc.

(E) Averaged PCP vectors in WT (n = 9 discs, 1,801 clones). Region-specific color coding of averaged PCP nematics or averaged PCP vectors: green, ventral wing pouch; yellow, dorsal wing pouch; orange, hinge; red, Wg-expressing region; cyan, region of Ptc upregulation.

(F) Locally averaged PCP nematics from a Fmi stained disc overlaid on Wg + Ptc staining to indicate compartment boundaries.

Scale bar represents 50 μm (see also Figure S1).

proximal wing near the anterior wing margin orient toward the margin rather than away from the hinge (Figures S2D and S2E). Near the AP boundary, hairs form swirling patterns (Figure S2E). Thus, Ft and Ds are required during larval growth to ensure that PCP vectors in the proximal wing orient away from the hinge.

The DV Boundary Organizer Orients PCP in the Central Wing Pouch

Notch and Wg signaling at the DV boundary organize growth and patterning in the developing wing. These pathways maintain each other via a positive feedback loop; Notch induces transcription of Wg at the DV interface, and Wg signaling upregulates expression of the Notch ligands Delta (Dl) and Serrate (Ser) adjacent to the Wg expression domain [11–15], further activating Notch signaling at the DV boundary. To study how the DV boundary organizer affects PCP, we ectopically expressed Ser along the AP boundary with *ptc*-Gal4 (*ptc* > *Ser*). In the ventral compartment, Ser induces two adjacent stripes of Wg expression, which then upregulate Dl expression in flanking regions (dorsally, Fringe prevents Notch activation by Ser [16]; Figure 3A; Figure S3D′). The posterior Wg and Dl stripes are distinct, but the anterior stripes are broader due to the graded activity of *ptc*-Gal4 (Figure 3A; Figure S3D′). In these discs, the ventral compartment overgrows along the AP boundary, parallel to the ectopic "organizers" (Figure 3A).

PCP nematics and vectors near the posterior Wg/Dl stripes are organized similarly to those flanking the normal DV boundary—running parallel to the stripe and turning sharply outside this region to orient toward the ectopic organizer (Figure 3A; Figures S3C and S3C′). PCP nematics anterior to the ectopic Ser stripe run parallel to it over larger distances before turning sharply, consistent with the broader Wg/Dl expression in this region (Figure 3A). In resulting adult wings, hairs orient toward the ectopic wing margin that forms along the AP boundary (Figures S3A and S3B). Ectopically expressing Wg along the AP boundary also generates an ectopic organizer that reorients growth and PCP (Figure 3B).

To ask how loss of the DV boundary organizer affected PCP, we used a temperature-sensitive allele of *wg* that blocks Wg secretion (wg^{TS}) or we populated wings with *wg* null mutant clones [17]. Loss of Wg signaling severs the feedback loop with Notch such that both decay [14]. We quantified PCP nematics in wg^{TS} discs shifted to the restrictive temperature shortly after the second to third-instar transition (earlier, Wg is required to specify the wing pouch [18]). wg^{TS} discs have smaller wing pouches than WT and are missing a large fraction of the central region of the pouch where polarity orients perpendicular to the DV boundary (compare Figure 3C to 3H). Polarity still orients away from the hinge, thus the PCP pattern in wg^{TS} discs appears more radial (i.e., oriented toward the center of the wing pouch) (Figure 3C; Figures S3E–S3F″). Analogously, adult wings populated by *wg* null clones are missing those regions of the distal wing blade where hairs normally point perpendicular to the wing margin (Figure 3E). The remaining proximal tissue is normally polarized except at its distal

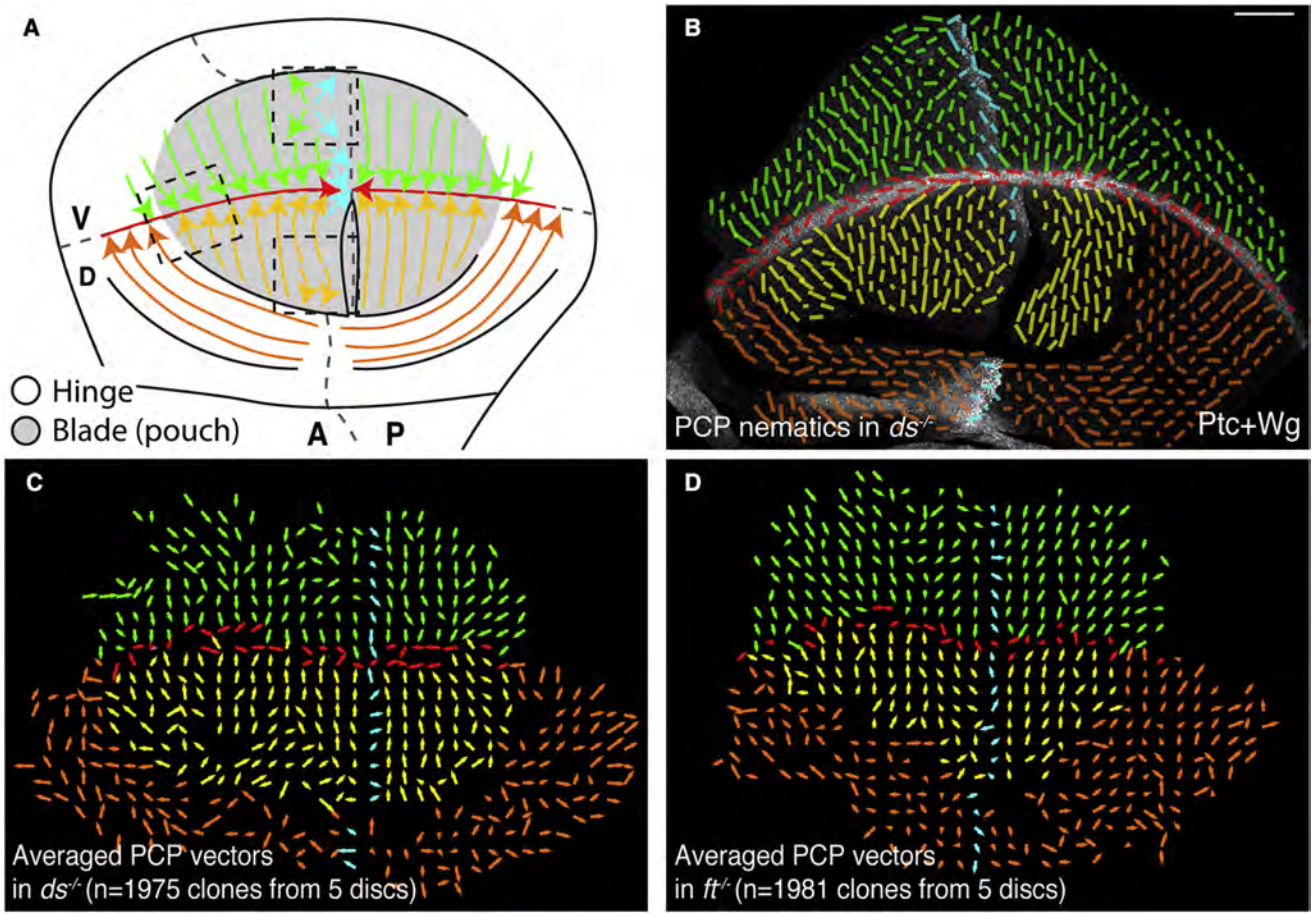

Figure 2. *ft* and *ds* Mutant Discs Have Similar PCP Defects

(A) Cartoon showing PCP in *ft* and *ds* mutants (compare to Figure 1C). Regions with PCP defects are boxed and shown at higher magnification in Figures S2A–S2C′.

(B) Locally averaged PCP nematics based on Fmi staining in a ds^{05142} mutant wing disc overlaid on Wg + Ptc staining.

(C and D) Averaged PCP vectors in ds^{05142} (C; n = 5 discs, 1,975 clones) and in $ft^{4}/ft^{G\text{-}rv}$ (D; n = 5 discs, 1,981 clones).

Scale bar represents 50 μm (B) (see also Figure S2).

edges (Figures 3E and 3G). Here, polarity deflects from the proximal-distal axis to parallel the edge of the wing. Normally, hair polarity in the wing blade parallels the margin only in proximal regions, where Ft/Ds influences polarity (Figures 3D and 3F). Thus, the DV organizer is needed to orient PCP in distal regions perpendicular to the margin. Ft/Ds is required for a complementary subset of the PCP pattern in the proximal wing. Their influences largely reinforce each other (i.e., away from the hinge and toward the DV boundary or wing margin) except where the hinge and wing margin intersect. Here, loss of one signaling system expands the influence of the other.

Wg is distributed in a graded fashion and is a ligand for Frizzled (Fz) [19, 20]. Thus, it could bias the PCP pattern directly, e.g., by asymmetrically inhibiting interactions between Fz, Strabismus (Stbm), and Fmi or causing Fz internalization. If so, uniform Wg overexpression should prevent intracellular polarization or reduce cortical localization of PCP proteins. To investigate this, we overexpressed Wg uniformly (*C765 > wg::HA*; Figure S3I). Uniform Wg expression elongates the wing pouch parallel to the AP boundary (Figure 3I). It broadens the pattern of Dl expression, such that sharp Dl stripes at the DV boundary are lost, but Dl expression remains excluded from the Hh signaling domain anterior to the AP boundary (Figure 3I; Figure S3D″). Fmi and EGFP::Pk polarize robustly in these discs (Figure 3I; Figures S3H, S3J, and S3K); thus, the Wg gradient does not act directly on PCP proteins to induce or orient polarity. However, the pattern of PCP vectors and nematics is altered. PCP points away from the hinge (rather than perpendicular to the DV boundary) over larger distances compared to WT and then turns sharply to face the DV boundary in the middle of the wing pouch (compare Figure 3H to 3I). Because specific alterations in the PCP pattern are induced by uniform Wg overexpression, Wg protein distribution does not directly specify the new PCP pattern.

Hh Signaling Interfaces Orient PCP near the AP Boundary

To identify signals that influence the PCP pattern near the AP boundary, we examined the effects of uniform high-level expression of Dpp and Hh, two morphogens that form graded distributions near the AP boundary. Uniform Dpp expression does not influence the magnitude of PCP or the range over which PCP deflects toward the AP boundary (Figure 4A; Figure S4C). Interestingly, uniform Hh expression dramatically increases the range over which PCP deflects toward the AP boundary (Figure 4B; Figure S4D), suggesting that Hh is important for this aspect of the pattern. However it clearly indicates

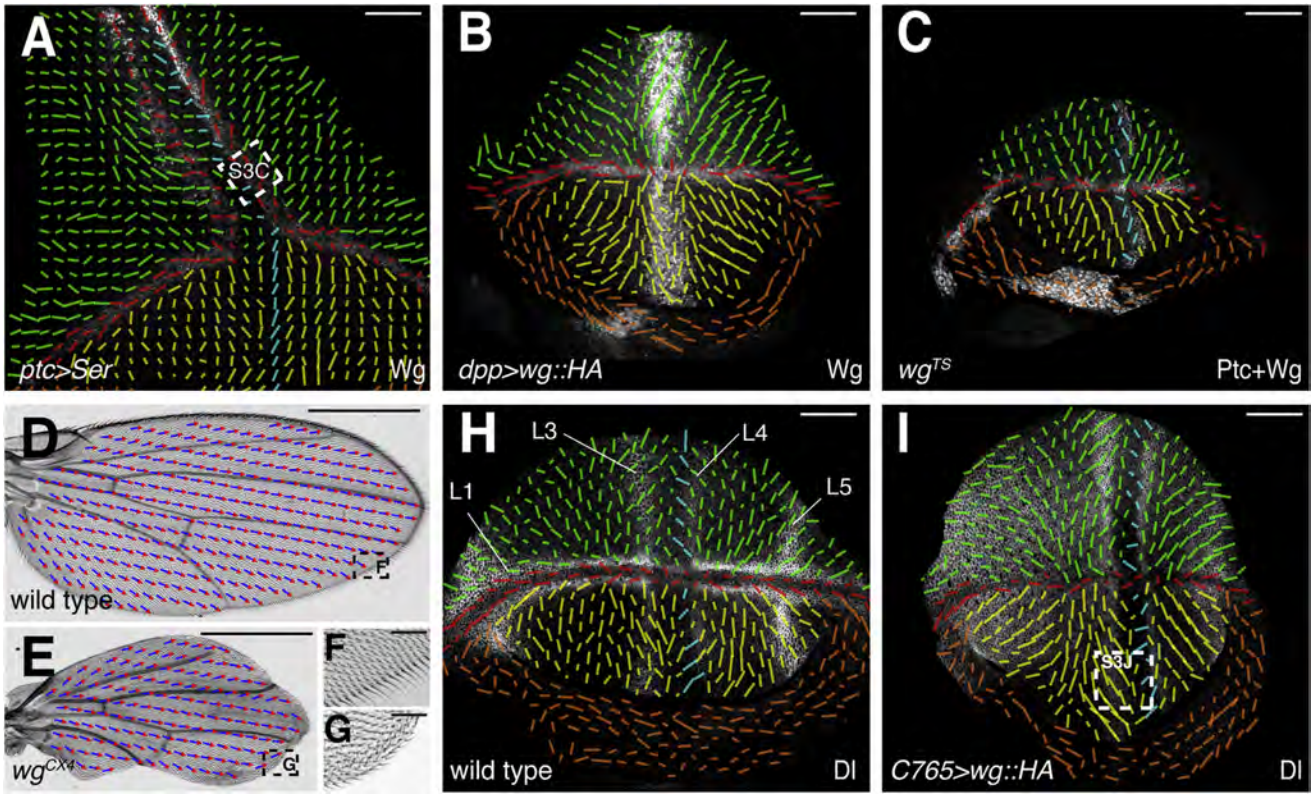

Figure 3. The DV Organizer Orients PCP in the Central Region of the Wing Pouch

(A) Locally averaged PCP nematics from a disc in which Ser expression is driven along the AP boundary under the control of *ptc*-Gal4 *(ptc > Ser)*. PCP nematics are overlaid on Wg staining. Box indicates the region analogous to that shown in Figures S3C and S3C′.

(B) Locally averaged PCP nematics from a disc expressing HA-tagged Wg along the AP boundary under the control of *dpp*-Gal4 (*dpp > wg::HA*). PCP nematics are overlaid on Wg staining.

(C) Locally averaged PCP nematics in a wg^{TS} disc overlaid on Wg and Ptc staining. Unsecreted Wg is still detected, but its expression is beginning to decay, confirming that Notch signaling is compromised.

(D–G) Hair polarity vectors calculated from tiled bright-field images of adult wings in WT (D) and *ubx-Flp;* wg^{CX4} *FRT40 / Minute FRT40* (E). Adult wings consisting predominantly of *wg* mutant tissue were generated by giving *wg* mutant cells a growth advantage using the Minute system. Red arrowheads indicate hair orientation. Boxed regions are enlarged in (F) and (G).

(F and G) Hair polarity at the distal posterior wing margin in WT (F) and *ubx-Flp;* wg^{CX4} *FRT40 / Minute FRT40* (G).

(H) Locally averaged PCP nematics of a WT disc overlaid on Dl staining. Dl upregulation in longitudinal veins (L1, L3, L4, L5) is indicated.

(I) Locally averaged PCP nematics in *C765 > wg::HA* overlaid on Dl staining. Boxed region corresponds to Figure S3J.

Locally averaged PCP nematics in (A–C), (H), and (I) based on Fmi staining. Scale bars represent 50 μm (A–C, F–I), and 500 μm (D and E) (see also Figure S3).

that PCP vectors are not oriented directly by the graded distribution of Hh or by the graded activity of Hh signaling, because both are uniformly high in the anterior compartment of Hh overexpressing discs (Figure S4B). We therefore considered whether the apposition of cells with very different levels of Hh signaling might produce sharp bends in the PCP pattern. In WT discs, Hh signaling levels change at two interfaces: one along the AP boundary and one along a parallel line outside the region of highest Hh signaling where Ptc is upregulated. PCP vectors orient parallel to the AP boundary in the cells posterior to it, deflect toward the boundary anteriorly, and then reorient sharply outside of this region to align parallel to the AP boundary (Figures 1E, 1F, and 3H). Discs uniformly overexpressing Hh have only one signaling discontinuity (at the AP boundary), because Hh signaling is high throughout the anterior compartment (Figures S4A and S4B). This could explain why PCP in these discs remains deflected toward the AP boundary over longer distances.

To test this, we generated clones mutant for the Hh receptor Ptc, which constitutively activate signaling in the absence of ligand [21]. Quantifying PCP nematics in these discs reveals reproducible patterns of polarity reorientation at interfaces between WT and ptc^- tissue. In WT tissue adjacent to ptc^- clones, PCP aligns parallel to the clone interface. Due to the typical clone shape, this orientation is often consistent with the normal PCP pattern. However, PCP also aligns parallel to ptc^- clones in regions where this is not so (Figure 4C; Figure S4F). Thus, ptc^- clones exert a dominant effect on adjacent WT tissue. In contrast, on the mutant side of the clone interface, polarity tends to orient perpendicular to the interface (Figure 4C; Figure S4E). Thus, apposition of high and low levels of Hh signaling causes a sharp bend in the PCP pattern. Corresponding polarity reorientation by ptc^- clones is also seen in adult wings (Figures 4D and 4D′). Thus, Hh signaling has two effects in WT discs: within the Hh signaling domain, it deflects PCP toward the AP boundary, and just outside the Hh signaling domain, it orients PCP parallel to the AP boundary. In this region, the tendency for polarity to align parallel to Hh signaling interfaces is consistent with the orientation of polarity toward the DV boundary and away from the

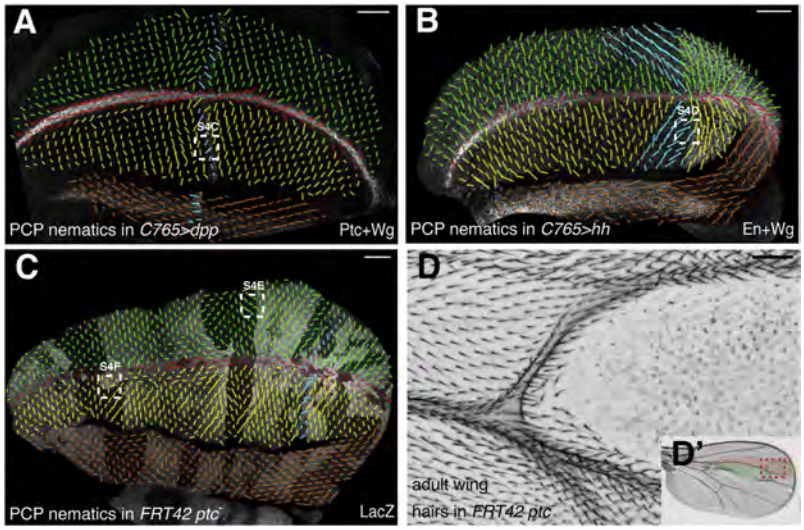

Figure 4. Hh Orients PCP Near the AP Boundary

(A–C) Locally averaged PCP nematics in *C765 > dpp* (A), *C765 > hh* (B), and *ubx-Flp; FRT42 ptc⁻ / FRT42 lacZ* (C) overlaid on Wg+Ptc (A), Wg+En (B), or lacZ (C) staining of the same disc. Cyan indicates anterior nematics that deflect toward the AP boundary.

(D) Hair polarity in an adult wing around a *ptc⁻* clone. *ptc⁻* cells are labeled by *shavenoid*, which stunts wing hairs. Clone position is indicated by shading in (D′). The clone populates both dorsal (green) and ventral (red) surfaces of the blade. *ptc⁻* clones induce veins in adjacent WT tissue. Hairs parallel the veins that surround the clone.

Scale bars represent 50 μm (see also Figure S4).

hinge. Thus, these three polarity cues reinforce each other throughout much of the wing pouch, making the global PCP pattern robust.

The PCP Pattern Is Not Directly Specified by Gradients

Simulations have highlighted the difficulty of establishing long-range polarity alignment in a large field of cells from an initially disordered arrangement [22, 23]. The pattern typically becomes trapped in local energy minima, forming swirling defects. Introducing a small bias in each cell removes such defects—this has been an attractive argument for the involvement of large-scale gradients in orienting PCP. The graded distribution of Ds along the proximal-distal axis (orthogonal to the hinge-pouch interface) suggested a plausible candidate for such a signal [24]. Strikingly, the Ds expression gradient gives rise to intracellular polarization of both Ft and Ds, and the recruitment of the atypical myosin Dachs to the distal side of each cell [25, 26]. Nevertheless, most of the PCP defects in *ft* mutants can be rescued by uniform overexpression of a truncated Ft version that cannot interact with Ds [27, 28], and PCP defects in *ds* mutants can be rescued by uniform overexpression of Ds [6, 28, 29]. Moreover, blocking overgrowth through removal of *dachs* also suppresses PCP phenotypes in both mutants [25, 26]. The remaining disturbances in PCP in each of these backgrounds are restricted to very proximal regions, both in adult wings and the wing disc. Thus, the graded distribution of Ds does not provide a direct cue to orient PCP over long distances; rather, it appears to be important only locally near the hinge. Furthermore, we show here that the two other key signaling pathways that contribute to the global PCP pattern in the disc do not act directly through long-range gradients. How do these signals specify the PCP pattern, if not through gradients? Simulations in the vertex model have suggested that long-range polarity can be established in the absence of global biasing cues if PCP is allowed to develop during growth. PCP easily aligns in a small system, and globally aligned polarity can then be maintained as the system grows [6]. Such a model obviates the necessity of long-range biasing cues like gradients, at least to maintain long-range alignment of PCP domains. Our finding that a global PCP pattern develops early during growth of the wing makes this idea plausible. It may be that a combination of local signals at the different organizer regions specifies the vector orientation of PCP when the disc is still small, and that the pattern is maintained during growth. This may explain why loss-of-function studies have failed to identify the signaling pathways at the AP and DV boundaries as important organizers of the PCP pattern.

In addition to local signals, the orientation of growth may provide additional cues that help shape the PCP pattern. Simulating the interplay between PCP and growth in the vertex model showed that oriented cell divisions and cell rearrangements orient PCP either parallel or perpendicular to the axis of tissue elongation, depending on parameters [6]. Interestingly, each of the signaling pathways that influence PCP in the disc also influences the disc growth pattern. Wg/Notch signaling at the DV boundary drives growth parallel to the DV boundary (Figures 3A and 3B; [8, 30]), consistent with the pattern of clone elongation at the DV boundary [31]. Growth near the AP boundary, where Hh signaling is most active, is oriented parallel to the AP boundary [30]. This behavior probably reflects oriented cell rearrangements rather than oriented cell divisions [32]. Finally, Ft and Ds orient growth away from the hinge [8, 9]. Suppressing overgrowth in *ft* or *ds* mutant wings by altering downstream components of the Hippo pathway rescues normal PCP except in the most proximal regions of the wing [25, 26, 33]. Thus, altered growth orientation may contribute to the PCP defects seen in *ft* and *ds* mutants.

Growth orientation reflects the orientation of both cell divisions and neighbor exchanges, and these can each exert different effects on the axis of PCP [6]. Understanding the influence of local growth patterns on PCP will require a quantitative description of the patterns of cell divisions and rearrangements in the disc. More refined simulations incorporating local differences in the orientation of cell divisions and rearrangements will allow us to explore how planar polarity patterns can be guided by different growth patterns.

Experimental Procedures

A summary of fly lines, antibodies, and immunohistochemical protocols is provided in the Supplemental Information. Imaging of entire wing discs at cellular resolution was performed with an Olympus FV-1000 confocal microscope with a programmable stage (further details in the Supplemental Information).

Quantification of Polarity Vectors and Nematics

Cells were segmented based on E-Cadherin staining as described previously [6]. PCP nematics were calculated as described [6], except that the

tensor components were normalized by the cell contour sum PCP intensity (see Supplemental Information).

PCP vectors $\vec{p}$ were computed individually for each EGFP::Pk clone (Figure 1B). They are defined as follows:

$$\vec{p} = -\frac{\sum_i \vec{n_i} I_i}{\sum_i I_i}, \quad \text{(Eq. 1)}$$

where the sums run over all cell boundaries *i* between clonal cells and non-clonal cells. $\vec{n_i}$ is the unit vector normal to cell boundary *i*, pointing away from the clone. I_i is the sum of the pixel intensities of cell boundary *i*. The vector defined in Equation 1 points away from high Pk intensity and by implication toward high Fz intensity (Figure 1B).

To average polarity patterns over many discs, we used the compartments boundaries and the interface between the hinge and pouch to define a coordinate system for each disc quadrant. Clone position and vector polarity are mapped to an average wing disc using these coordinate systems (see Supplemental Information).

Quantification of Hair Polarity

Using bright-field images of adult wings, we calculated nematics from local anisotropies of pixel intensity correlations. This nematic provides an axis of local polarity throughout the wing. Manually specifying the vector direction within a small region, we iteratively determine the vector direction in the whole wing (see Supplemental Information).

Supplemental Information

Supplemental Information includes four figures and Supplemental Experimental Procedures and can be found with this article online at doi:10.1016/j.cub.2012.04.066.

Acknowledgments

We are thankful to Christian Dahmann, Elisabeth Knust, Jean-Paul Vincent, Ken Irvine, Konrad Basler, the Bloomington Stock Center, and Developmental Studies Hybridoma Bank for providing fly strains and antibodies. We gratefully acknowledge David Strutt and his laboratory for sharing fly lines and results prior to publication and Raphael Etournay for providing a macro to record and stitch adult wings. We thank Natalie Dye, Raphael Etournay, and Pavel Tomancak for critical comments on the manuscript. This work was funded by the Max-Planck-Gesellschaft and by a grant to S.E. from the European Research Council.

Received: February 21, 2012
Revised: April 4, 2012
Accepted: April 27, 2012
Published online: June 21, 2012

References

1. Bayly, R., and Axelrod, J.D. (2011). Pointing in the right direction: new developments in the field of planar cell polarity. Nat Rev Genet *12*, 385–391.
2. Simons, M., and Mlodzik, M. (2008). Planar cell polarity signaling: from fly development to human disease. Annu. Rev. Genet. *42*, 517–540.
3. Strutt, H., and Strutt, D. (2009). Asymmetric localisation of planar polarity proteins: Mechanisms and consequences. Semin. Cell Dev. Biol. *20*, 957–963.
4. Lawrence, P.A., Struhl, G., and Casal, J. (2007). Planar cell polarity: one or two pathways? Nat. Rev. Genet. *8*, 555–563.
5. Strutt, D. (2009). Gradients and the specification of planar polarity in the insect cuticle. Cold Spring Harb Perspect Biol *1*, a000489.
6. Aigouy, B., Farhadifar, R., Staple, D.B., Sagner, A., Röper, J.C., Jülicher, F., and Eaton, S. (2010). Cell flow reorients the axis of planar polarity in the wing epithelium of Drosophila. Cell *142*, 773–786.
7. Ng, M., Diaz-Benjumea, F.J., Vincent, J.P., Wu, J., and Cohen, S.M. (1996). Specification of the wing by localized expression of wingless protein. Nature *381*, 316–318.
8. Baena-López, L.A., Baonza, A., and García-Bellido, A. (2005). The orientation of cell divisions determines the shape of Drosophila organs. Curr. Biol. *15*, 1640–1644.
9. Mao, Y., Tournier, A.L., Bates, P.A., Gale, J.E., Tapon, N., and Thompson, B.J. (2011). Planar polarization of the atypical myosin Dachs orients cell divisions in Drosophila. Genes Dev. *25*, 131–136.
10. Thomas, C., and Strutt, D. (2012). The roles of the cadherins Fat and Dachsous in planar polarity specification in Drosophila. Dev. Dyn. *241*, 27–39.
11. Diaz-Benjumea, F.J., and Cohen, S.M. (1995). Serrate signals through Notch to establish a Wingless-dependent organizer at the dorsal/ventral compartment boundary of the Drosophila wing. Development *121*, 4215–4225.
12. Couso, J.P., Knust, E., and Martinez Arias, A. (1995). Serrate and wingless cooperate to induce vestigial gene expression and wing formation in Drosophila. Curr. Biol. *5*, 1437–1448.
13. de Celis, J.F., and Bray, S. (1997). Feed-back mechanisms affecting Notch activation at the dorsoventral boundary in the Drosophila wing. Development *124*, 3241–3251.
14. Micchelli, C.A., Rulifson, E.J., and Blair, S.S. (1997). The function and regulation of cut expression on the wing margin of Drosophila: Notch, Wingless and a dominant negative role for Delta and Serrate. Development *124*, 1485–1495.
15. Hayward, P., Kalmar, T., and Arias, A.M. (2008). Wnt/Notch signalling and information processing during development. Development *135*, 411–424.
16. Panin, V.M., Papayannopoulos, V., Wilson, R., and Irvine, K.D. (1997). Fringe modulates Notch-ligand interactions. Nature *387*, 908–912.
17. Piddini, E., and Vincent, J.P. (2009). Interpretation of the wingless gradient requires signaling-induced self-inhibition. Cell *136*, 296–307.
18. Klein, T. (2001). Wing disc development in the fly: the early stages. Curr. Opin. Genet. Dev. *11*, 470–475.
19. Bhanot, P., Brink, M., Samos, C.H., Hsieh, J.C., Wang, Y., Macke, J.P., Andrew, D., Nathans, J., and Nusse, R. (1996). A new member of the frizzled family from Drosophila functions as a Wingless receptor. Nature *382*, 225–230.
20. Chen, C.M., and Struhl, G. (1999). Wingless transduction by the Frizzled and Frizzled2 proteins of Drosophila. Development *126*, 5441–5452.
21. Chen, Y., and Struhl, G. (1996). Dual roles for patched in sequestering and transducing Hedgehog. Cell *87*, 553–563.
22. Amonlirdviman, K., Khare, N.A., Tree, D.R., Chen, W.S., Axelrod, J.D., and Tomlin, C.J. (2005). Mathematical modeling of planar cell polarity to understand domineering nonautonomy. Science *307*, 423–426.
23. Burak, Y., and Shraiman, B.I. (2009). Order and stochastic dynamics in Drosophila planar cell polarity. PLoS Comput. Biol. *5*, e1000628.
24. Ma, D., Yang, C.H., McNeill, H., Simon, M.A., and Axelrod, J.D. (2003). Fidelity in planar cell polarity signalling. Nature *421*, 543–547.
25. Brittle, A., Thomas, C., and Strutt, D. (2012). Planar Polarity Specification through Asymmetric Subcellular Localization of Fat and Dachsous. Curr. Biol. *22*, 907–914.
26. Mao, Y., Rauskolb, C., Cho, E., Hu, W.L., Hayter, H., Minihan, G., Katz, F.N., and Irvine, K.D. (2006). Dachs: an unconventional myosin that functions downstream of Fat to regulate growth, affinity and gene expression in Drosophila. Development *133*, 2539–2551.
27. Matakatsu, H., and Blair, S.S. (2006). Separating the adhesive and signaling functions of the Fat and Dachsous protocadherins. Development *133*, 2315–2324.
28. Matakatsu, H., and Blair, S.S. (2012). Separating planar cell polarity and Hippo pathway activities of the protocadherins Fat and Dachsous. Development *129*, 1498–1508.
29. Matakatsu, H., and Blair, S.S. (2004). Interactions between Fat and Dachsous and the regulation of planar cell polarity in the Drosophila wing. Development *131*, 3785–3794.
30. Milán, M., Campuzano, S., and García-Bellido, A. (1996). Cell cycling and patterned cell proliferation in the Drosophila wing during metamorphosis. Proc. Natl. Acad. Sci. USA *93*, 11687–11692.
31. Resino, J., Salama-Cohen, P., and García-Bellido, A. (2002). Determining the role of patterned cell proliferation in the shape and size of the Drosophila wing. Proc. Natl. Acad. Sci. USA *99*, 7502–7507.
32. Landsberg, K.P., Farhadifar, R., Ranft, J., Umetsu, D., Widmann, T.J., Bittig, T., Said, A., Jülicher, F., and Dahmann, C. (2009). Increased cell bond tension governs cell sorting at the Drosophila anteroposterior compartment boundary. Curr. Biol. *19*, 1950–1955.
33. Feng, Y., and Irvine, K.D. (2007). Fat and expanded act in parallel to regulate growth through warts. Proc. Natl. Acad. Sci. USA *104*, 20362–20367.